ISBN: 978-3-95450-231-8 ISSN: 2673-5490 doi: 10.18429/JACoW-IPAC2023-MOPL147

ULTRA-THIN FILM YTTRIA ENHANCED GOLD PHOTOCATHODES

C. Benjamin[1,*], R. Valizadeh[1], T. C. Q. Noakes[1]. ASTeC, STFC Daresbury Laboratory
Sci-Tech Daresbury, Warrington, UK
G. R. Bell, University of Warwick, Coventry, United Kingdom
[1]also at the Cockcroft Institute, Sci-Tech Daresbury, Warrington, UK

Abstract

The performance requirements for next generation electron accelerators put ever increasing demand on the photocathode performance, where it fundamentally limits the achievable beam quality. Metal photocathodes are limited by their high work function and relatively low quantum efficiency, necessitating the use of high powered deep UV lasers. Metal oxide thin film interfaces have been shown to reduce the work function of the underlying metal photocathode, whilst maintaining the ease of use, high durability and fast response time. This leads to an improvement in quantum efficiency and spectral response to desirable incident laser sources. We present the characterisation of a thin film yttria (Y_2O_3) enhanced Au photocathode at various film thicknesses. Quantum efficiencies were measured at 265 nm along with surface compositions via X-ray photoelectron spectroscopy.

INTRODUCTION

Next generation accelerators, such as, X-ray free electron lasers (XFEL) and ultrafast relativistic electron diffraction (UED) systems both require specialised photocathodes to drive them. XFELs demand a high brightness electron sources with a focus on relatively high beam currents. In contrast, UEDs require high coherence, low beam emittance, and short pulse width. In both cases, high quantum efficiency (QE) and low intrinsic emittance is required. The former allows for higher beam currents or reduces power demand from the drive laser and the latter improves beam brightness as poor beam emittance cannot be improved further along the accelerator. These requirements highlight the need for the investigation and characterisation of novel photocathode materials. The photoemissive properties of a photocathode are predominantly governed by the surface properties, surface roughness and work function (WF), as they strongly influence both the QE and intrinsic emittance.

It has been shown in recent years, by first-principles calculations, that ultra-thin metal oxide films at the surface of a metal photocathode can dramatically improve the QE[1, 2]. This is principally from work function reduction induced by a strong dipole moment, which itself is brought about by three main mechanisms: interfacial charge transfer, electrostatic compression and surface reconstruction mechanisms [3]. Experimentally, it has been confirmed that an epitaxial MgO film approximately one monolayer thick reduces the WF of Ag(100) by around 1 eV. This WF reduction consequently improves the QE and the spectral response of the underlying metal photocathode[4]. An additional benefit is an improvement of the photocathode's resistance to contamination by gases, which its surface can be exposed to during operation in a photoinjector.

In this work, we investigate a novel metal oxide enhanced metal photocathode system, in the form of yttria (Y_2O_3) thin films grown on a gold (Au) photocathode. The QE at 265 nm is investigated with respect to the thickness of Y_2O_3 film. X-ray photoelectron spectroscopy (XPS) was utilised to confirm stoichiometry of the oxide thin film deposition and to calculate the thickness.

EXPERIMENTAL DETAILS

Sample Preparation

A 15 mm diameter Au foil cathode was cleaned *in situ* using cleaning cycles of Kr^+ bombardment at 5 keV beam energy for 20 mins and annealing. Cleanliness of the cathode was confirmed using XPS, showing no surface contaminants, such as adventitious carbon and oxygen species. The Au cathode was then subject to a series of Y_2O_3 depositions by ion beam sputtering deposition. In this method, a Y target was sputtered with Kr^+ with a beam energy of 5 keV, measuring a target current of 30 μA without any secondary electron suppression. The Au cathode was positioned 30 mm away from the target. Afterwards, O_2 was admitted into the chamber to oxidise the yttrium film. XPS spectra and quantum efficiency measurements were acquired between deposition cycles.

Surface Characterisation

XPS spectra were acquired using a non-monochromated Al Kα x-ray source and a Thermo Alpha 110 hemispherical analyser. The analyser transmission function was determined experimentally using the technique described by Ruffiuex *et al.* [5], and the effective WF of the analyser was calibrated using the Fermi edge of Ag. Survey and core region spectra were acquired with a pass energy of 50 eV and 20 eV respectively. XPS data analysis was conducted using the CasaXPS software package [6].

Quantum Efficiency Measurements

QE measurements were taken using a 265 nm (FWHM 13 nm) LED with a power of 0.3 mW incident to the sample surface, measuring the drain current of the sample under a high voltage extraction electrode.

* Christopher.Benjamin@stfc.ac.uk

ISBN: 978-3-95450-231-8 ISSN: 2673-5490 doi: 10.18429/JACoW-IPAC2023-MOPL147

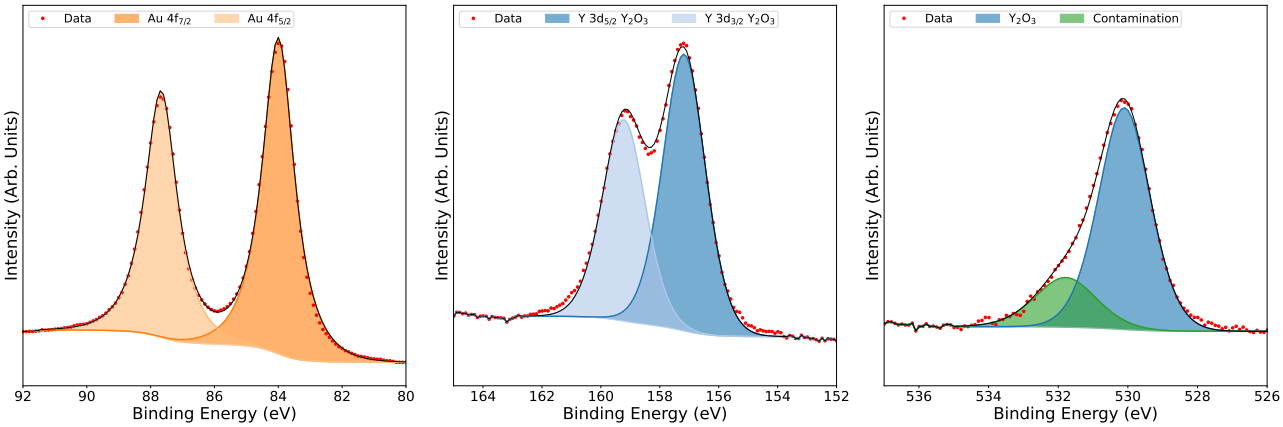

(a) Au 4f (b) Y 3d (c) O 1s

Figure 1: XPS core region spectra of: Au 4f, O 1s and Y 3d, corresponding to a total deposition time of 155 minutes.

EXPERIMENTAL RESULTS

The Au substrate was chosen due to its chemical stability and robustness when exposed to oxygen during the deposition cycles, which could have potentially led to degradation of QE in typically used metal photocathodes, such as, copper. After cleaning cycles the QE of the Au foil, at 265 nm, was measured to be 1.02×10^{-5}. Once the baseline was established, Y_2O_3 was deposited in four subsequent depositions of lengths: 5, 30, 120 and then 60 mins. Figure 1 shows the XPS spectra for the Au 4f, Y 3d and O 1s core regions after a total deposition time of 155 mins, the final deposition where the Au 4f is still observable. As expected, the Au 4f spectrum (figure 1a) is unchanged throughout the deposition process with no observable change in full-width half maximum (FWHM) of the fitted components or shift in binding energy (BE). The Y 3d (figure 1b) core region displays two components corresponding to the Y $3d_{5/2}$ and Y $3d_{3/2}$ due to spin-orbit splitting. The BE of the Y $3d_{5/2}$ was measured to be 157.2 eV, in agreement with literature values for Y_2O_3[7]. No components at a lower BE corresponding to metallic Y were observed suggesting an oxide film.

Table 1 shows the atomic percentages of the Au, Y and O using XPS after each deposition and the calculated thickness of the Y_2O_3 film using using the thickogram method outlined by Cumpson [8]. Figure 2 displays the QE of the Au as a function of the thickness of the Y_2O_3 film is shown. After a deposition length of 5 min an incomplete film was deposited, this still resulted in a QE increased by over a factor of 3. At around a monolayer thick (1 nm) the QE increased by a factor of 4 compared to the clean Au foil. The final two depositions, with thicknesses calculated to be 3 nm and 6 nm, results in a QE lower than the Au foil. This suggests an increase in the Y_2O_3 film thickness above a few monolayers leads to a decrease in the QE, below that of the clean Au.

DISCUSSION

As shown in Table1, the atomic concentrations derived from the core region spectra of the XPS suggests that the deposition method employed did not result in a stoichiometric oxide film with a slight amount of excess Y present, which could be, in the form of metallic Y or sub-oxides. This is due to fact the Y was oxidised after ion beam deposition and not during. This may have resulted in a small contribution to the QE from any metallic Y present. However, as discussed previously, the Y 3d core region (figure 1b) has no observable metallic component and therefore the excess Y must be below background levels detectable in our XPS system.

In terms of photocathode performance, we observed a significant increase in QE at 265 nm with the inclusion of the ultra-thin Y_2O_3 film. After a total deposition length of 35 mins (around 1 nm), we achieved a factor of four increase in the QE relative to the clean Au photocathode. Increasing the thickness of the Y_2O_3 film above 2.5 nm resulted in a reduction in QE, lower than the clean Au photocathode. Since photoemission is occurring at the Au photocathode, as the thickness of the Y_2O_3 film increases the probability of photoemitted electrons escaping through the Y_2O_3 to vacuum decreases. This results in a lower QE which counters the decrease of the WF reduction occurring at the Au/Y_2O_3 interface.

CONCLUSION

In this paper, we have investigated a novel photocathode system. We have experimentally shown that the inclusion of a ultra thin Y_2O_3 film about a few monolayers results in a QE enhancement of the underlying Au foil. A further increase in thickness hinders the QE. This is in agreement with previously discussed work, where the surface dipole induced at the metal oxide metal interface results in a WF reduction, improving the the photoemission response to higher wavelengths and QE at the at the same wavelength. This significant improvement in the QE and the robust nature of

ISBN: 978-3-95450-231-8 ISSN: 2673-5490 doi: 10.18429/JACoW-IPAC2023-MOPL147

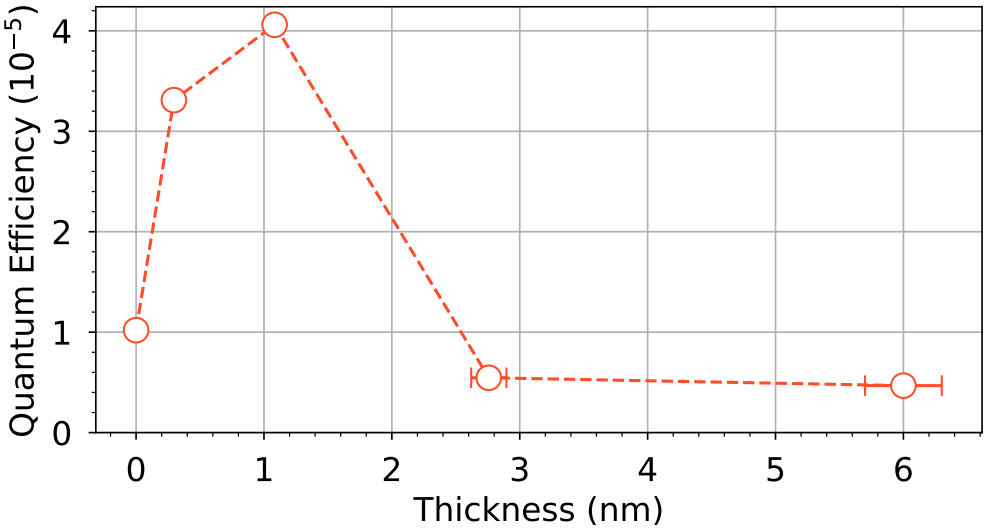

Figure 2: Measured quantum efficiency of a Au photocathode with respect to the deposited Y_2O_3 film thickness.

Total Deposition [mins]	XPS Au 4f [at %]	XPS Y 3d [at %]	XPS O 1s [at %]	Y_2O_3 Thickness [nm]
0	100	0	0	-
5	73	13	14	0.3
35	41	29	30	1.1
155	16	43	41	2.8
215	0	57	43	>6

Table 1: Atomic percentages of each element present obtained through XPS and the calculated thickness of the Y_2O_3 after each deposition run.

both Y_2O_3 and Au opens an avenue of research into ultra thin Y_2O_3 film enhance metal photocathodes as a candidate for future photocathode applications

FUTURE WORK

Further characterisation of these photocathodes is paramount to fully understand the photoemissive properties observed. *In situ* ultraviolet photoelectron spectroscopy is required to determine the change in WF and the resulting spectral response observed due to the inclusion of the oxide thin film. Futhermore, characterisation of the mean tranverse energy ascertaining the intrinsic emittance of the photocathode which requires a specialised measurement systems, such as the tranverse energy spread spectrometer located at Daresbury Laboratory.

REFERENCES

[1] V. Chang, T. C. Q. Noakes, and N. M. Harrison, "Work function and quantum efficiency study of metal oxide thin films on ag(100)," *Physical Review B*, vol. 97, p. 155 436, 15 2018. doi:10.1103/PhysRevB.97.155436

[2] T. Jaouen, G. Jézéquel, G. Delhaye, B. Lépine, P. Turban, and P. Schieffer, "Work function shifts, schottky barrier height, and ionization potential determination of thin mgo films on ag(001)," *Applied Physics Letters*, vol. 97, p. 232 104, 23 2010. doi:10.1063/1.3525159

[3] J. Goniakowski and C. Noguera, "Polarization and rumpling in oxide monolayers deposited on metallic substrates," *Phys. Rev. B*, vol. 79, p. 155 433, 15 2009. doi:10.1103/PhysRevB.79.155433

[4] C. Benjamin *et al.*, "Enhanced performance of an ag(100) photocathode by an ultra-thin mgo film," *Journal of Applied Physics*, vol. 132, no. 19, p. 195 303, 2022. doi:10.1063/5.0124528

[5] P. Ruffieux *et al.*, "Experimental determination of the transmission factor for the omicron ea125 electron analyzer," *Review of Scientific Instruments*, vol. 71, p. 3634, 2000. doi:10.1063/1.1313798

[6] N. Fairley *et al.*, "Systematic and collaborative approach to problem solving using x-ray photoelectron spectroscopy," *Applied Surface Science Advances*, vol. 5, p. 100 112, 2021. doi:10.1016/j.apsadv.2021.100112

[7] A. V. Naumkin, A. Kraut-Vass, S. W. Gaarenstroom, and C. J. Powell, *Nist x-ray photoelectron spectroscopy database*, NIST Standard Reference Database Number 20, National Institute of Standards and Technology, Gaithersburg MD, 20899 (2000), doi:10.18434/T4T88K, (retrieved [01/02/2022]).

[8] P. J. Cumpson, "The thickogram: A method for easy film thickness measurement in xps," *Surface and Interface Analysis*, vol. 29, no. 6, pp. 403–406, 2000. doi:10.1002/1096-9918